New Experimental Data and Mechanistic Studies on the Bromate−Dual Substrate−Dual Catalyst Batch Oscillator

István Szalai, Krisztina Kurin-Csörgei, Viktor Horváth, and Miklós Orbán*

Department of Inorganic and Analytical Chemistry, L. Eötvös University, P.O. Box 32, H-1518 Budapest 112, Hungary

Received: January 13, 2006; In Final Form: March 17, 2006

The bromate−hypophosphite−acetone−Mn(II)−$Ru(bpy)_3^{2+}$ batch oscillator was recently suggested for studying two-dimensional pattern formation. The system meets all major requirements that are needed for generation of good quality traveling waves in a thin solution layer. The serious drawback of using the system for studying temporal and spatial dynamical phenomena is its unknown chemical mechanism. In order to develop a mechanism that explains the observed long-lasting batch oscillations the bromate−hypophosphite−acetone−Mn(II)−$Ru(bpy)_3^{2+}$ oscillator was revisited. We studied the dynamics both in the total system and in some composite reactions, and kinetic measurements were carried out in three subsystems. From the new experimental results we concluded that the two oscillatory sequences observed in the full system are originated from two oscillatory subsystems, the Mn(II)-catalyzed bromate−hypophosphite−acetone and the $Ru(bpy)_3^{2+}$-catalyzed bromate−bromoacetone reactions. Here we propose a mechanism which is capable of simulating the dynamical features that appeared in the complex system.

Introduction

The reaction between bromate and hypophosphite ions in the presence of a Mn(II) catalyst was reported long ago to show oscillations in the redox potential and in the light absorbance, if the bromine formed during the reaction was removed from the system by an inert gas flow or by adding acetone.[1] In a typical experiment only a few (5−10) oscillations can be observed (Figure 1a). These oscillations appear in a finite range of gas flow rate or of acetone concentration. We found later that introducing a small amount of a second catalyst (10^{-5}–10^{-4} mol/dm^3 $Ru(bpy)_3SO_4$, ferroin, or diphenylamine) into the Mn(II)-catalyzed bromate−hypophosphite short-lived oscillatory system generates long-lasting oscillations.[2] In most cases, the long-lasting oscillations begin after an induction period (Figure 1b). The bromate−hypophosphite−acetone−Mn(II)−$Ru(bpy)_3^{2+}$ system is ideally suited for studying pattern evolution. It exhibits long-lasting batch oscillations, it does not produce gaseous product or precipitate, and it gives rises to color oscillations in a stirred batch reactor and well visible patterns in an unstirred solution layer. Both phenomena are maintained for many (>5) hours.

To facilitate modeling of the rich temporal and spatial dynamical behaviors observed in the title reaction requires a simple but reliable chemical mechanism. Here we suggest a mechanism based on our new experimental observations and kinetic measurements performed in some subsystems of the complex reaction.

Experimental Section

H_2SO_4 (Chemolab 96%), $NaH_2PO_2 \cdot H_2O$ (Sigma), KBr (Reanal p.a.), $NaBrO_3$ (Fluka p.a.), $MnSO_4 \cdot H_2O$, $Ru(bpy)_3Cl_2 \cdot 6H_2O$ (Aldrich), acetone (Fisher), and bidistilled water were used to prepare the working solutions. $Ru(bpy)_3SO_4$ was obtained by converting the chloride salt to the sulfato form using the recipe suggested by Gao and Försterling.[3] Stock solutions of $Ru(bpy)_3^{3+}$ were prepared from the stock solutions of $Ru(bpy)_3^{2+}$

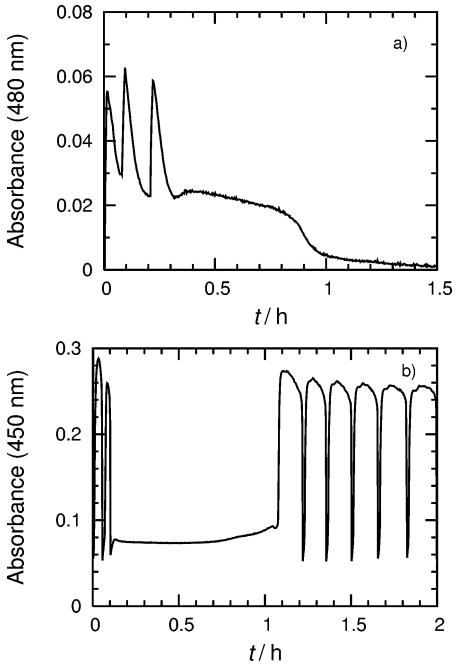

Figure 1. Oscillations in the absorbance measured in the BrO_3^-−H_3PO_2−acetone−Mn(II) system (a) in the absence and (b) in the presence of 5×10^{-5} mol/dm^3 $Ru(bpy)_3^{2+}$. Initial concentrations: $[BrO_3^-] = 0.02$ mol/dm^3, $[H_3PO_2] = 0.1$ mol/dm^3, [acetone] = 0.1 mol/dm^3, $[H_2SO_4] = 1.0$ mol/dm^3, [Mn(II)] = 0.003 mol/dm^3. The main absorbing species at $\lambda = 480$ nm: Mn(III) ($\epsilon = 120$ mol^{-1} dm^{-3} cm^{-1}) and Br_2 ($\epsilon = 60$ mol^{-1} dm^{-3} cm^{-1}). At $\lambda = 450$ nm: $Ru(bpy)_3^{2+}$ ($\epsilon = 14\,500$ mol^{-1} dm^{-3} cm^{-1}), $Ru(bpy)_3^{3+}$ ($\epsilon = 150$ mol^{-1} dm^{-3} cm^{-1}), and Br_2 ($\epsilon = 120$ mol^{-1} dm^{-3} cm^{-1}). The color oscillates between pink and colorless in panel a and between yellow and green in panel b.

* To whom correspondence should be addressed. E-mail: orbanm@ludens.elte.hu.

10.1021/jp0602575 CCC: $33.50
Published on Web 04/15/2006

by oxidation with solid PbO_2 followed by filtration on a fritted glass. The $Ru(bpy)_3^{3+}$ solutions were stored in darkness and used within 1 h. A $Mn_2(SO_4)_3$ stock solution was prepared by reacting a known amount of $KMnO_4$ with a 50-fold excess of $MnSO_4$ in 2 mol/dm^3 sulfuric acid.

The spectra for kinetic measurements were taken on Milton Roy 3000 and Agilent 8452 diode array spectrophotometers equipped with quartz cells (path length 1 cm, volume 2 mL). In the cells the temperature was kept at 20.0 (±0.1) °C, and the solutions were mixed by magnetic stirrer.

The simulations were done with the program XPPAUT.[4] The parameter estimations were carried out by the MULTIMRQ program using the Marquardt method.[5] Fitted parameters are given at the 95% significance level.

Results

Effect of Stirring Intensity on the Dynamics of the BrO_3^-−H_3PO_2−Acetone−Mn(II) Oscillatory System. Pojman and co-workers[6] observed a strong effect of stirring on the behavior of the short-lived bromate−hypophosphite−Mn(II)−acetone oscillator. No oscillations occurred in the system unless a gas/liquid interface was present. The absorption of the bromine on the Teflon stirring bar or on the wall of the reactor also influenced the dynamics. They concluded that the system is extremely sensitive to the rate of removal of the volatile species. They detected bromoacetone and bromine in the gas phase above the reaction mixture using the GC/MS method.

In agreement with Pojman's observations we found that the number of the oscillations depends on the reactor geometry and the stirring rate, and under similar conditions the number of oscillations increases when the intensity of the stirring increases. Surprisingly, applying quite intense stirring (high stirring rate and relatively big Teflon coated stirrer bar) we observed long-lasting oscillations in the absent of any second catalyst. The oscillations in the bromate−hypophopshite−Mn(II)−acetone system at a high stirring rate are presented in Figure 2.

This long-lasting batch oscillator cannot, of course, be utilized for studying pattern formation due to its requirement of strong stirring. However, the importance of bromine removal for maintaining the sustained-like oscillations in the bromate−dual substrate−dual catalyst system was considered in our mechanistic studies.

Dynamics in the BrO_3^-−Acetone−$Ru(bpy)_3^{2+}$ Subsystem. In order to clarify the role of the second catalyst in the title reaction, experiments were performed in the bromate−acetone−$Ru(bpy)_3^{2+}$ subsystem to check the possibility of BZ-type (bromide-controlled) oscillations in this composite reaction. In a BZ-type oscillator the reaction between the brominated organic intermediate and the oxidized form of the catalyst produces bromide ions, the inhibitor of the autocatalytic bromate−bromous acid reaction in the oscillatory kinetics.

Rastogi and Misra[7] showed earlier that oscillations can occur in the Ce(IV)- or Mn(II)-catalyzed bromate−acetone reaction at high temperature (50 °C) and at high acetone concentration (3.4 M). At room temperature or below (20 °C) we have not found oscillations in the presence of any BZ catalyst including $Ru(bpy)_3^{2+}$. We supposed that at room temperature the bromination of the acetone is too slow to generate enough bromoacetone, the intermediate that is needed for production of a sufficient amount of bromide in the oxidation reaction of the bromoacetone. However, when additional bromoacetone was produced by applying bromide ion perturbation in the bromate−acetone−$Ru(bpy)_3^{2+}$ system, oscillations appeared at 20 °C. The result is shown in Figure 3. The bromide ions injected at the times indicated by the arrows produced elementary bromine in the system, which brominated the acetone in a slow reaction. The processes are described by eqs 1 and 2 and recorded in Figure 3 as the first peaks after the perturbations. The oscillations start after the bromine is consumed by acetone. The increasing amount of added bromide yields more and more bromoacetone, which results in longer and longer oscillatory sequences. For example, when 7×10^{-3} M bromide was added to the system in Figure 3, the oscillations lasted for 3 h.

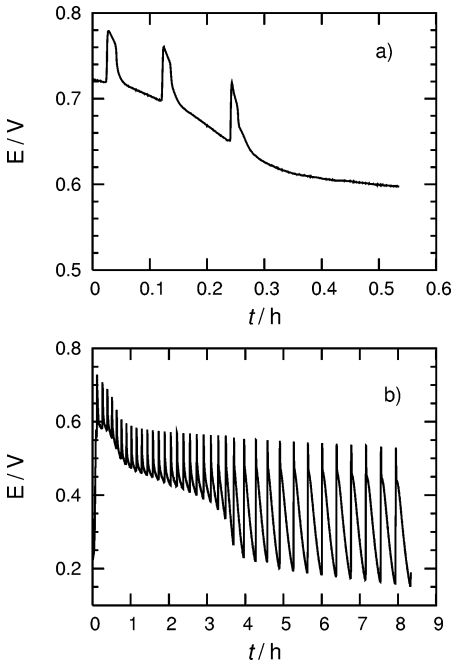

Figure 2. Effect of stirring rate on duration of the oscillations in the potential of a Pt vs Hg/Hg_2SO_4/saturated K_2SO_4 electrode pair in the BrO_3^-−H_3PO_2−acetone−Mn(II) system. Initial concentrations: $[BrO_3^-]$ = 0.02 mol/dm^3, $[H_3PO_2]$ = 0.075 mol/dm^3, [acetone] = 0.09 mol/dm^3, $[H_2SO_4]$ = 1.0 mol/dm^3, [Mn(II)] = 0.0036 mol/dm^3. Stirring rate: (a) 300 rpm, (b) 900 rpm.

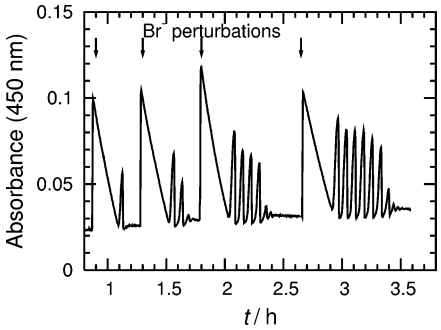

Figure 3. Oscillations in the absorbance recorded in the BrO_3^-−acetone−$Ru(bpy)_3^{2+}$ system after perturbation with Br^- ions. Initial concentrations: $[BrO_3^-]$ = 0.02 mol/dm^3, [acetone] = 0.1 mol/dm^3, $[H_2SO_4]$ = 1.0 mol/dm^3, $[Ru(bpy)_3]^{2+}$ = 5×10^{-5} mol/dm^3. In each perturbation $[Br^-]$ = 0.001 mol/dm^3 was added at the times shown by the arrows.

$$BrO_3^- + 5Br^- + 6H^+ \rightarrow 3Br_2 + 3H_2O \quad (1)$$

$$Br_2 + Ac \rightarrow BrAc + H^+ + Br^- \quad (2)$$

We prepared bromoacetone in a separate experiment by mixing a known amount of bromide and acetone with an excess

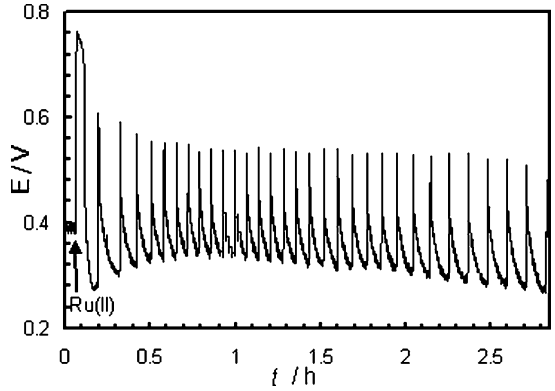

Figure 4. Sustained-like oscillations in the bromate−bromoacetone−$Ru(bpy)_3^{2+}$ subsystem. Initial concentrations: $[BrO_3^-] = 0.073$ mol/dm^3, [acetone] = 0.2 mol/dm^3, $[H_2SO_4] = 1.16$ mol/dm^3, $[Br^-] = 0.106$ mol/dm^3. Time of bromination: 4 h. Calculated concentrations after bromination: $[BrO_3^-] = 0.02$ mol/dm^3, [bromoacetone] = 0.16 mol/dm^3, $[H_2SO_4] = 1.0$ mol/dm^3, $[Br^-] = 0$ mol/dm^3, [acetone] = 0.04 mol/dm^3 (this amount of acetone falls below the limit when oscillations can occur in the bromoacetone-free system). The oscillations were initiated by adding $[Ru(bpy)_3]^{2+} = 5 \times 10^{-5}$ mol/dm^3. Stirring rate: 600 rpm. Temperature: 25 °C.

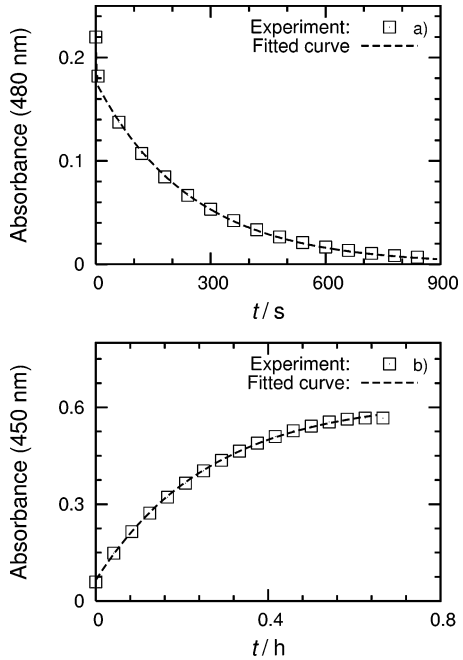

Figure 5. The absorbance vs time curves in the oxidation of H_3PO_2 by (a) Mn(III) and (b) $Ru(bpy)_3^{3+}$. Experimental conditions: (a) $[H_3PO_2] = 0.1$ mol/dm^3, $[H_2SO_4] = 1.0$ mol/dm^3, [Mn(III)] = 0.002 mol/dm^3. At $\lambda = 480$ nm the main absorbing species are Mn(III) and $MnH_3PO_2^{3+}$ complex. (b) $[H_3PO_2] = 0.5$ mol/dm^3, $[H_2SO_4] = 1.0$ mol/dm^3, $[Ru(bpy)_3]^{3+}] = 4 \times 10^{-5}$ mol/dm^3. At $\lambda = 450$ nm the main absorbing species are $Ru(bpy)_3^{2+}$ and $Ru(bpy)_3^{3+}$.

(and known amount) of bromate in the presence of 1 M H_2SO_4. The bromination of the acetone (the disappearance of the brown color of bromine) was completed within 3−4 h. From the stoichiometry of eqs 1 and 2 and using the initial concentrations shown in Figure 4 the [BrAc] was calculated to be 0.16 mol/dm^3. The concentration of BrO_3^- and H_2SO_4 in the mixture after the bromination was close to the initial concentrations of Figure 3. When a small amount of $Ru(bpy)_3^{2+}$ catalyst was introduced into the mixture, oscillations in the potential of the Pt electrode and in the color started, and the seemingly undamped oscillations were recorded for $3^1/_2$ h (see Figure 4). The oscillations showed strong sensitivity to the stirring rate. High amplitude potential oscillations (∼150 mV) appeared at 300−700 rpm, the amplitude decreased to half at 200 rpm, and the oscillations stopped below 100 rpm.

The appearance of the oscillations in the bromide perturbed bromate−acetone−$Ru(bpy)_3^{2+}$ reaction mixture suggests that the reaction between bromoacetone and $Ru(bpy)_3^{3+}$ catalyst (eq 3) provides an effective source of bromide ions for generating a BZ-type oscillatory behavior.

$$\mathrm{Ru(III)} + \mathrm{BrAc} \rightarrow \mathrm{Br}^- + \mathrm{products} \qquad (3)$$

Kinetics of Some Composite Reactions. *Oxidation of H_3PO_2 by Mn(III) Ions.* The reaction was studied in $[H_2SO_4] = 1$ mol/dm^3 at different initial concentrations of Mn(III) ($1 \times 10^{-3} - 5 \times 10^{-3}$ mol/dm^3) and NaH_2PO_2 (0.05−0.2 mol/dm^3). In 1 mol/dm^3 sulfuric acid the NaH_2PO_2 is present in the form of H_3PO_2 ($pK_a = 2.0$). A typical absorbance vs time curve is shown in Figure 5a. A similar mechanism as proposed by Caroll and Thomas[8] for the oxidation of H_3PO_2 with Ce(IV) was assumed to exist in the Mn(III)−H_3PO_2 reaction. The mechanism is represented by steps RI−RIII.

$$\mathrm{Mn(III)} + \mathrm{H_3PO_2} \leftrightarrows [\mathrm{MnH_3PO_2}]^{3+} \qquad (\mathrm{RI})$$

$$v_\mathrm{I}^\mathrm{f} = k_\mathrm{I}^\mathrm{f}[\mathrm{Mn(III)}][\mathrm{H_3PO_2}]$$

$$v_\mathrm{I}^\mathrm{r} = k_\mathrm{I}^\mathrm{r}[\mathrm{MnH_3PO_2}^{3+}]$$

$$[\mathrm{MnH_3PO_2}]^{3+} \rightarrow \mathrm{Mn(II)} + \mathrm{H_2PO_2}^\bullet + \mathrm{H}^+ \qquad (\mathrm{RII})$$

$$v_\mathrm{II} = k_\mathrm{II}[\mathrm{MnH_3PO_2}^{3+}]$$

$$2\mathrm{H_2PO_2}^\bullet + \mathrm{H_2O} \rightarrow \mathrm{H_3PO_2} + \mathrm{H_3PO_3} \qquad (\mathrm{RIII})$$

$$v_\mathrm{III} = k_\mathrm{III}[\mathrm{H_2PO_2}^\bullet]^2$$

The first step in the mechanism is the formation of a complex between Mn(III) and H_3PO_2 (RI). Reduction of Mn(III) occurs in RII, which is the rate determining step in the overall process. RIII is the disproportion of $H_2PO_2^\bullet$ radicals which yields reagent H_3PO_2 and end product H_3PO_3.

We used nonlinear parameter estimation to evaluate k_II and $K_\mathrm{I} = k_\mathrm{I}^\mathrm{f}/k_\mathrm{I}^\mathrm{r}$ from the spectrophotometric measurements. If RIII is assumed to be a fast reaction ($k_\mathrm{III} = 3 \times 10^9$ mol^{-1} dm^{-3} s^{-1}), then for K_I and k_II, 29(±2) mol^{-1} dm^{-3} and 5.6(±0.1) × 10^{-3} s^{-1}, respectively, are derived. These values are in good agreement with the results of Zhang and Field.[9] The sum of the reactions RI−RIII is designated as R12 in our model suggested to describe the oscillatory behavior in the total system.

$$2\mathrm{Mn(III)} + \mathrm{H_3PO_2} + \mathrm{H_2O} \rightarrow 2\mathrm{Mn(II)} + \mathrm{H_3PO_3} + 2\mathrm{H}^+ \qquad (\mathrm{R12})$$

$$v_{12} = k_{12}K[\mathrm{Mn(III)}]_\mathrm{t}[\mathrm{H_3PO_2}]/(1 + K[\mathrm{H_3PO_2}])$$

$$[\mathrm{Mn(III)}]_\mathrm{t} = [\mathrm{Mn(III)}] + [\mathrm{MnH_3PO_2}^{3+}]$$

$$k_{12} = k_\mathrm{II}, \quad K = K_\mathrm{I}$$

Oxidation of H_3PO_2 by $Ru(bpy)_3^{3+}$ Ions. The reaction was studied in $[H_2SO_4] = 1$ mol/dm^3 at different initial concentrations of H_3PO_2 (0.5−1 mol/dm^3). A typical absorbance vs time

TABLE 1: Model for the $BrO_3^- - H_3PO_2 -$ Acetone $- Mn(II) - Ru(bpy)_3^{2+}$ Oscillatory System[a]

R1	$BrO_3^- + Br^- + 2H^+ \rightarrow HBrO_2 + HOBr$	$v_1 = k_1[BrO_3^-][Br^-]$
R2	$HBrO_2 + Br^- + H^+ \rightarrow 2HOBr$	$v_2 = k_2[HBrO_2][Br^-]$
R3	$BrO_3^- + HBrO_2 + 3H^+ + 2Mn(II) \rightarrow 2HBrO_2 + 2Mn(III) + H_2O$	$v_3 = k_3[HBrO_2][BrO_3^-]$
R4	$2HBrO_2 \rightarrow BrO_3^- + HOBr + H^+$	$v_4 = k_4[HBrO_2]^2$
R5	$HOBr + Br^- + H^+ \leftrightarrows Br_2 + H_2O$	$v_5 = k_5^f[HOBr][Br^-] - k_5^b[Br_2]$
R6	$Br_2 + H_3PO_2 + H_2O \rightarrow 2Br^- + H_3PO_3 + 2H^+$	$v_6 = k_6[Br_2][H_3PO_2]$
R7	$BrO_3^- + H_3PO_2 + H^+ \rightarrow HBrO_2 + H_3PO_3$	$v_7 = k_7[BrO_3^-][H_3PO_2]$
R8	$HBrO_2 + H_3PO_2 \rightarrow HOBr + H_3PO_3$	$v_8 = k_8[HBrO_2][H_3PO_2]$
R9	$HOBr + H_3PO_2 \rightarrow Br^- + H_3PO_3 + H^+$	$v_9 = k_9[HOBr][H_3PO_2]$
R10	$Br_2 \rightarrow fBr^- + fBrAc$	$v_{10} = k_{10}[Br_2]$
R11	$Ru(III) + BrAc \rightarrow Br^-$	$v_{11} = k_{11}[Ru(III)]$
R12	$2Mn(III) + H_3PO_2 + H_2O \rightarrow 2Mn(II) + H_3PO_3 + 2H^+$	$v_{12} = k_{12}K[Mn(III)][H_3PO_2]/(1 + K[H_3PO_2])$
R13	$2Ru(III) + H_3PO_2 + H_2O \rightarrow 2Ru(II) + H_3PO_3 + 2H^+$	$v_{13} = k_{13}[Ru(III)][H_3PO_2]$
R14	$Mn(III) + Ru(II) \rightarrow Mn(II) + Ru(III)$	$v_{14} = k_{14}([Ru]_T - [Ru(III)])[Mn(III)]$

[a] Abbreviations: BrAc ≡ bromoacetone, Ru(III) ≡ $[Ru(bpy)_3]_3^{3+}$, Ru(II) ≡ $[Ru(bpy)_3]_3^{2+}$, $[Ru]_T = [Ru(II)] + [Ru(III)]$. The variables in the model are $[BrO_3^-]$, $[H_3PO_2]$, $[Br^-]$, $[HBrO_2]$, [HOBr], $[Br_2]$, [Mn(III)], [Ru(III)]. In $[H_2SO_4] = 1.0$ mol/dm^3 used in the experiments the $[H^+] = 1.29$ mol/dm^3.[15] This value is included in the rate constants of v_1, v_2, v_3, v_5, and v_7. k_{11} is a pseudo-first-order rate constant that includes [BrAc].

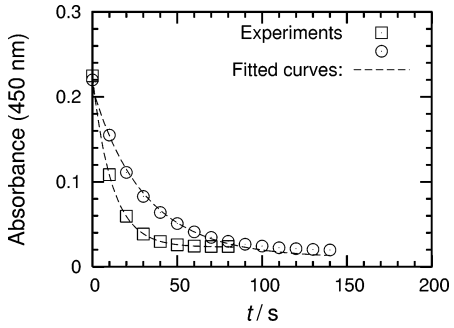

Figure 6. Oxidation of $Ru(bpy)_3]^{2+}$ by Mn(III). Experimental conditions: $[H_2SO_4] = 1.0$ mol/dm^3, $[Ru(bpy)_3^{2+}] = 1.5 \times 10^{-5}$ mol/dm^3, $[Mn(III)] = 1.0 \times 10^{-4}$ mol/dm^3 (⊙), $[Mn(III)] = 2.0 \times 10^{-4}$ mol/dm^3(⊡).

curve is shown in Figure 5b. The reaction follows second-order kinetics (eq R13).

$$2Ru(bpy)_3^{3+} + H_3PO_2 + H_2O \rightarrow 2Ru(bpy)_3^{2+} + H_3PO_3 + 2H^+ \quad (R13)$$

$$v_{13} = k_{13}[Ru(bpy)_3^{3+}][H_3PO_2]$$

$$k_{13} = 2.1(\pm 0.4) \times 10^{-3}\ \text{mol}^{-1}\ \text{dm}^3\ \text{s}^{-1}$$

Oxidation of $Ru(bpy)_3^{2+}$ by Mn(III) Ions. The oxidation of $Ru(bpy)_3^{2+}$ by Mn(III) in $[H_2SO_4] = 1$ mol/dm^3 is a fast reaction. The reaction was studied at different initial concentrations of Mn(III) (5×10^{-5} to 2×10^{-4} mol/dm^3). In the parameter estimation it was taken into account that the stock solution of Mn(III) contained a high amount of Mn(II) ions. At $\lambda = 450$ nm the decrease in $[Ru(bpy)_3]^{2+}$ vs time was followed (Figure 6). The equilibrium constant of the reaction was calculated from redox potential data: E^0 (Mn(III)/Mn(II)) = 1.51 V,[10] E^0 ($Ru(bpy)_3^{3+}/Ru(bpy)_3^{2+}$) = 1.27 V.[11] The fit between the calculated curve and the measured data is good. The reaction takes place as a second-order step (R14):

$$Mn(III) + Ru(bpy)_3^{2+} \leftrightarrows Mn(II) + Ru(bpy)_3^{3+} \quad (R14)$$

$$k_{14}^f = 360(\pm 5)\ \text{mol}^{-1}\ \text{dm}^3\ \text{s}^{-1}$$

$$K_{14} = 1.1 \times 10^4$$

Mechanistic Model

Our aim was to build a relatively simple chemical model to explain the major features of the dynamical behavior observed in the bromate$-H_3PO_2-$acetone−dual catalyst system, considering that the dynamics is rather complex: it is sensitive to stirring, and five input components (bromate, hypophosphite, acetone, Mn(II), $Ru(bpy)_3^{2+}$) and at least three volatile species (bromine, acetone, bromoacetone) are involved. The model we suggest is presented in Table 1. The parameters used in the simulations are shown in Table 2.

TABLE 2: Parameters Used in the Simulations

	parameters	refs
R1	$k_1 = 2.0$ mol^{-1} dm^3 s^{-1}	1
R2	$k_2 = 3.2 \times 10^6$ mol^{-1} dm^3 s^{-1}	13
R3	$k_3 = 80$ mol^{-2} dm^6 s^{-1}	*a*
R4	$k_4 = 4.38 \times 10^3$ mol^{-1} dm^3 s^{-1}	14
R5	$k_5^f = 1 \times 10^{10}$ mol^{-1} dm^3 s^{-1}	13
	$k_5^b = 80$ s^{-1}	
R6	$k_6 = 1.04$ mol^{-1} dm^3 s^{-1}	9
R7	$k_7 = 1 \times 10^{-5}$ mol^{-1} dm^3·s^{-1}	9
R8	$k_8 = 10$ mol^{-1} dm^3 s^{-1}	9
R9	$k_9 = 0.8$ mol^{-1} dm^3 s^{-1}	9
R10	adjustable	
R11	adjustable	
R12	$k_{12} = 5.6 \times 10^{-3}$ s^{-1}, $K = 29$ mol^{-1} dm^{-3}	*b*
R13	$k_{13} = 2.1 \times 10^{-3}$ mol^{-1} dm^3 s^{-1}	*b*
R14	$k_{14} = 360$ mol^{-1} dm^3 s^{-1}	*b*

[a] Adjusted here. [b] Measured here.

Steps R1−R5 in the model represent the well-known Mn(II)-catalyzed oxybromine chemistry, which results in formation of bromine in reactions of R1 + R2 + 3 × R5. Bromine is consumed by hypophosphite in a slow process of R6 and by reaction with acetone in step R19a (see below). The next three steps (R7−R9) describe the oxidation of hypophosphite with bromine species:

$$BrO_3^- + 3H_3PO_2 \rightarrow Br^- + 3H_3PO_3 \quad (R7 + R8 + R9)$$

This overall process is a Landolt type clock reaction and autocatalytic for hydrogen and bromide ions.

There are two main routes of bromine removal in the system, a chemical and a physical route. Most important chemical removal of bromine is its reaction with acetone:[12]

$$Br_2 + Ac \rightarrow BrAc + H^+ + Br^- \quad (R19a)$$

$$v_{10a} = kk_E^f[Ac][Br_2]/(k_E^b + k[Br_2])$$

where k_E^f and k_E^b are the forward and backward rate constants of the enolization of acetone, and k is the rate constant of the

reaction between bromine and the enol form of acetone. In the experiments the bromine concentration is low and the concentration of acetone is relatively high; therefore the rate equation can be simplified as

$$v_{10a} = k_{10a}[Br_2]$$

$$k_{10a} = (kk_E^f/k_E^b)[Ac]$$

The second route implies the heterogeneous bromine removal by inert gas flow, by evaporation, or by adsorption on the stirrer bar and on the wall, etc. This process is expressed in step R19b:

$$Br_2 \rightarrow v_{10b} = k_{10b}[Br_2] \qquad \text{(R19b)}$$

In a typical experiment both routes are present. In the model, reaction R10 represents the overall removal of the bromine:

$$Br_2 \rightarrow fBr^- + fBrAc \qquad \text{(R19)}$$

$$v_{10} = k_{10}[Br_2]$$

$$k_{10} = k_{10a} + k_{10b}$$

We introduce factor *f*, which shows the ratio of the homogeneous chemical removal of bromine compared to the total removal:

$$f = v_{10a}/(v_{10a} + v_{10b})$$

In the absence of acetone $v_{10a} = 0$, $f = 0$ (no extra bromide formation can occur for lack of BrAc), and $k_{10} = k_{10b}$. In the case of pure homogeneous bromine removal $v_{10b} = 0$, $f = 1$, and $k_{10} = k_{10a}$. In a real experiment with acetone present the contribution of any heterogeneous process decreases the value of *f* and the stoichiometry of the bromide production in R10 falls between 0 and 1.

Step R11 in the model is the reaction between bromoacetone and $Ru(bpy)_3^{3+}$. Since bromoacetone is not a variable of the model, its concentration is included in the rate constant k_{11}. The next two reactions, R12 and R13, are the oxidation of hypophosphite by the oxidized form of the catalyst, and the last one, R14, is the reaction between the two catalysts. The overall mechanism contains 14 reactions and 8 variables.

Simulations and Discussions

The Effect of Bromine Removal on the Dynamics of the BrO_3^-−H_3PO_2−Acetone−Mn(II) System. The dynamics of the bromate−hypophosphite−Mn(II) oscillatory reaction was found to be very sensitive to the rate and the method of bromine removal. In the experiments oscillations appeared in a finite range of the acetone concentration, and the number of oscillations was highly sensitive to the rate of stirring (see Figure 2).

The number of oscillations predicted by the model strongly depends on the actual values of *f* and k_{10}. In Figure 7 the results of simulations are shown at a given value of k_{10} when $f = 1.0$ (solid line) and $f = 0.8$ (dashed line). At $f = 1.0$ (pure chemical removal of bromine) only a few oscillations appear. A small decrease in the value of *f* (contribution of physical processes to the bromine removal) induces an increase in the number of oscillations, similarly as in the experiments. By using bromate and hypophosphite as pool components, we calculated a phase diagram in the k_{10} vs *f* plane (Figure 8). The figure shows the oscillatory domain simulated at a given rate of total bromine removal (k_{10}) when the ratio of the physical and chemical removal (*f*) changes. At $f = 0$, which means there is no acetone in the system and just heterogeneous bromine escape occurs, the range of oscillations is very narrow. The strong sensitivity of the number of oscillations on the rate of bubbling N_2 gas in the bromate−hypophosphite−Mn(II) system was first demonstrated by Adamcikova and Sevcik.[1] When the relative rate of the homogeneous bromine removal is increased by addition of acetone (increasing the value of *f*), the range of oscillations increases, as in the experiments.

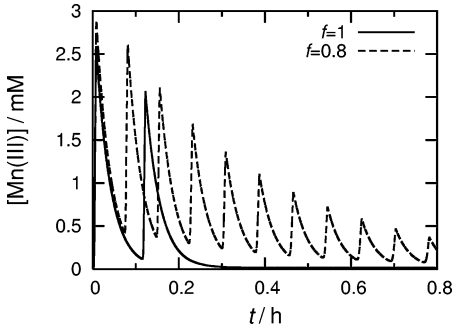

Figure 7. Simulated oscillations in the BrO_3^-−H_3PO_2−acetone−Mn(II) system (the second catalyst is absent) at different factors *f*. Initial concentrations: $[BrO_3^-] = 0.02$ mol/dm^3, $[H_3PO_2] = 0.1$ mol/dm^3. Parameters: $[H^+] = 1.29$ mol/dm^3, $k_{10} = 0.16$ s^{-1}, $f = 1$ (—) and $f = 0.8$ (- - -).

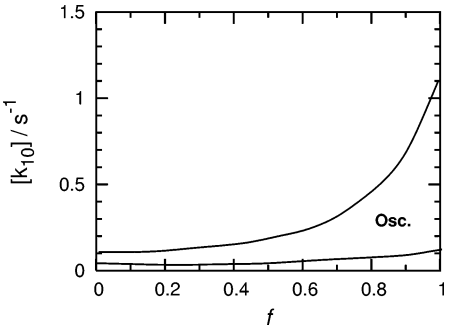

Figure 8. Simulated phase diagram of the bromate−H_3PO_2−acetone−Mn(II) system in the *f* vs k_{10} plane. Parameters: $[BrO_3^-] = 0.02$ mol/dm^3, $[H_3PO_2] = 0.1$ mol/dm^3, $[H^+] = 1.29$ mol/dm^3.

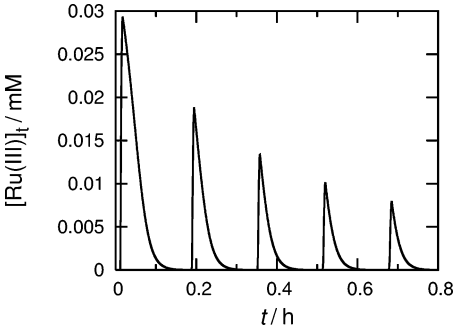

Figure 9. Simulated oscillations in the bromate−acetone−$Ru(bpy)_3^{2+}$ subsystem. Initial concentrations: $[BrO_3^-] = 0.02$ mol/dm^3, $[Br^-] = 1 \times 10^{-5}$ mol/dm^3. Parameters: $[H^+] = 1.29$ mol/dm^3, $[Ru]_T = 5 \times 10^{-5}$ mol/dm^3, $k_{10} = 0.5$ s^{-1}, $k_{11} = 2$ s^{-1}, and $f = 1$.

Oscillations in the BrO_3^-−Acetone−$Ru(bpy)_3^{2+}$ Subsystem. The model is capable of simulating the experimentally found oscillations in the bromate−acetone−$Ru(bpy)_3^{2+}$ subsystem as well. The results are shown in Figure 9. In the absence of hypophosphite our model works like an extended version of the Oregonator. The necessary conditions for the oscillations to occur are the removal of bromine and the appropriate rate of the bromide ion production in reaction R11. In the model k_{11} is a pseudo-first-order rate constant that includes the concentration

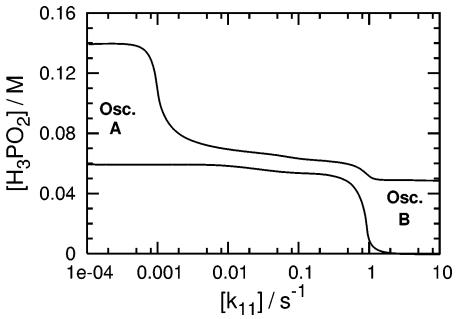

Figure 10. Simulated phase diagram of the bromate−hypophosphite−Mn(II)−$Ru(bpy)_3^{2+}$ system in the k_{11} vs $[H_3PO_2]$ plane. Here bromate and hypophosphite are pool components. Parameters: $[BrO_3^-]_0 = 0.02$ mol/dm^3, $[H^+]_0 = 1.29$ mol/dm^3, $[Ru]_T = 5 \times 10^{-5}$ mol/dm^3, $k_{10} = 0.5$ s^{-1}, $f = 1$.

of bromoacetone. To accomplish the second condition, the concentration of bromoacetone has to reach a critical value. This is the reason why the appearance of the oscillations required an induction time in the experiments.

Dynamics in the Total System. In the bromate−hypophosphite−acetone−dual catalyst system two sequences of oscillations were observed, a short-lived one which appeared shortly after mixing the reagents and a long-lived oscillation sequence which started after an induction time. The model in Table 1 simulates the two domains. In Figure 10 the two oscillatory domains (Osc. A and Osc. B) were calculated in the $[H_3PO_2]$ vs k_{11} plane, where $k_{11} = k'_{11}$[BrAc]. We believe that the substrate in the oscillator is H_3PO_2 in the part of Osc. A and BrAc in the part of Osc. B. In the system at the start the value of k_{11} is low (low concentration of BrAc), the $[H_3PO_2]$ is high, and the oscillatory domain simulated as Osc. A in Figure 10 corresponds to the short-lived oscillation in the bromate−hypophosphite−acetone−Mn(II) system. The oscillations in color between pink (from Mn(III)) and colorless are clearly seen during this stage of the reaction. As the reaction proceeds, the concentration of the hypophosphite decreases, while BrAc starts to accumulate and at a critical value of [BrAc] the bromate−BrAc−$Ru(bpy)_3^{2+}$ subsystem starts to oscillate (Osc. B). These oscillations are maintained as long as BrAc is produced in the Mn(II)-catalyzed reaction. The experimental observations and the results of simulations support the conclusion that the complex oscillatory pattern that was found in the bromate−hypophosphite−acetone−dual catalyst system is the result of an interaction between two internally coupled oscillators.

Acknowledgment. This work was financially supported by grants from the Hungarian Academy of Sciences (HAS) (OTKA No. T043743 and F034976).

References and Notes

(1) Adamcikova, L.; Sevcik, P. *Int. J. Chem. Kinet.* **1982**, *14*, 735. Sevcik, P.; Adamcikova, L. *Collect. Czech. Chem. Commun.* **1987**, *52*, 2125.; Quyang, Q.; Tam, W. J.; De Kepper, P.; McCormick, W. D.; Noszticzius, Z.; Swinney, H. L. *J. Phys. Chem.* **1987**, *91*, 2181.

(2) Orbán, M.; Kurin-Csörgei, K.; Zhabotinsky, A. M.; Epstein, I. R. *Faraday Discuss.* **2001**, *120*, 11.

(3) Gao, Y.; Försterling, H. D. *J. Phys. Chem.* **1995**, *99*, 8638.

(4) Ermentrout, B. *XPPAUT 5.41* Differential Equations Tool, www.math.pitt.edu/~bard/xpp/xpp.html (accessed 2005).

(5) Keszei, E. *MULTIMRQ* Multiple Nonlinear Fitting with Deconvolution, http://keszei.chem.elte.hu/femto/fit/englishprog.html (accessed 2005).

(6) Pojman, J. A.; Dedeaux, H.; Forberry, D. *J. Phys. Chem.* **1992**, *96*, 7331.

(7) Rastogi, R. P.; Misra, G. P. *Indian J. Chem. A* **1990**, *29A*, 1205.

(8) Caroll, R. L.; Thomas, L. B. *J. Am. Chem. Soc.* **1966**, *88*, 1376.

(9) Zhang, Y. X.; Field, R. J. *J. Phys. Chem.* **1990**, *94*, 7154.

(10) *CRC Handbook of Chemistry and Physics*, 50th ed.; The Chemical Rubber Co.: Cleveland, Ohio, 1970.

(11) Wayne, R. P. *Principles and Applications of Photochemistry*; Oxford University Press: Oxford, 1988.

(12) Keeffe, J. R.; Kresge, A. J.; Schepp, N. P. *J. Am. Chem. Soc.* **1988**, *110*, 1993.

(13) Försterling, H. D.; Murányi, S.; Schreiber, H. *Z. Naturforsch.* **1989**, *44a*, 555.

(14) Försterling, H. D.; Varga, M. *J. Phys. Chem.* **1993**, *97*, 7932.

(15) Robertson, E. B.; Dunford, H. B. *J. Am. Chem. Soc.* **1964**, *86*, 5080.